第4章

放射線療法

鹿間　直人・福田　護

言うまでもなく乳癌においては全身療法の役割は大きく，新規抗癌剤やホルモン療法，分子標的治療薬などが話題を集めている。固形癌において全身に広がった微小転移を制御できる有効な全身療法が行われた場合には，適切な局所療法を加えることで生存率の向上が期待できることが報告されており，有効な全身療法が登場している乳癌診療において局所療法としての放射線治療の役割はさらに重要となっている。

現在，患者の利便性を考慮し短期間で術後照射を終了させる乳房部分照射や全乳房短期照射は欧米を中心に研究が進んでおり，今後わが国の日常臨床でも普及するものと思われるが，解決しなければならない諸問題が内在している。今回は，このような治療法を日常臨床に導入するにあたり，注意しておかなければならないピットホールを中心に，お二人の先生方にご執筆をお願いした。

「乳癌診療ガイドライン」が発行され，現在改訂の時期にある。文献の抽出の際にはランダム化比較試験や大規模研究が重要視されるため海外からの論文が主に選択されており，今後わが国からの信頼性の高いエビデンスを発信する必要性が再確認された。乳房切除後の術後照射は二つの信頼性の高いランダム化比較試験で生存率の向上が証明され，わが国のガイドラインでも行うことが推奨されている。しかし，わが国の外科の先生方にはその必要性が十分に受け入れられておらず，術後照射の施行頻度は低い。人種差などが原因となり海外のエビデンスがわが国に当てはまらないためなのか，またエビデンスを臨床の現場に外挿する過程で何らかの問題があるのか，わが国発のエビデンスを持たない我々には解決し難い。しかし，このクリニカル・エビデンスギャップ(臨床とエビデンスの乖離)をいかに埋めていくかは臨床的に重要であり，田村先生には外科の立場からご自身の施設の成績も含めてご検討いただいた。

次々に新しい情報が発信される中，我々がその情報をどのように解釈し臨床の現場に取り入れていくかは重要な作業である。また，いまだ解決に至っていない事項に関しては，新たな研究課題であることは間違いない。

これからの乳癌診療
2008～2009

定価（本体6,000円＋税）

2008年3月31日　第1版第1刷発行

監　修　園尾博司
編　集　福田　護
　　池田　正
　　佐伯俊昭
　　鹿間直人

発行者　川井　弘光
発行所　金原出版株式会社
〒113-8687　東京都文京区湯島2-31-14
電話　編集 03（3811）7162
　　営業 03（3811）7184
FAX　03（3813）0288
振替　00120-4-151494
http://www.kanehara-shuppan.co.jp/

JCLS <㈱日本著作出版権管理システム委託出版物> ISBN 978-4-307-20239-8

印刷・製本：真興社

Int. J. Radiation Oncology Biol. Phys., Vol. 70, No. 2, pp. 626–633, 2008

0360-3016/08/$–see front matter

ELSEVIER

doi:10.1016/j.ijrobp.2007.09.053

PHYSICS CONTRIBUTION

IN VIVO DOSIMETRY OF HIGH-DOSE-RATE INTERSTITIAL BRACHYTHERAPY IN THE PELVIC REGION: USE OF A RADIOPHOTOLUMINESCENCE GLASS DOSIMETER FOR MEASUREMENT OF 1004 POINTS IN 66 PATIENTS WITH PELVIC MALIGNANCY

TAKAYUKI NOSE, M.D.,*† MASAHIKO KOIZUMI, M.D.,‡ KEN YOSHIDA, M.D.,§ KINJI NISHIYAMA, M.D.,‡ JUNICHI SASAKI,‡ TAKESHI OHNISHI,‡ TAKUYO KOZUKA, M.D.,* KOTARO GOMI, M.D.,* MASAHIKO OGUCHI, M.D.,* IORI SUMIDA, PH.D.,*† YUTAKA TAKAHASHI, PH.D.,† AKIRA ITO, PH.D.,† AND TAKASHI YAMASHITA, M.D.*†

*Department of Radiation Oncology, The Cancer Institute Hospital of the Japanese Foundation for Cancer Research, Tokyo, Japan; †Department of Physics, The Cancer Institute of the Japanese Foundation for Cancer Research, Tokyo, Japan; ‡Department of Radiation Oncology, Osaka Medical Center, Osaka, Japan; and §Department of Radiology, Osaka National Hospital, Osaka, Japan

Purpose: To perform the largest *in vivo* dosimetry study for interstitial brachytherapy yet to be undertaken using a new radiophotoluminescence glass dosimeter (RPLGD) in patients with pelvic malignancy and to study the limits of contemporary planning software based on the results.

Patients and Methods: Sixty-six patients with pelvic malignancy were treated with high-dose-rate interstitial brachytherapy, including prostate ($n = 26$), gynecological ($n = 35$), and miscellaneous ($n = 5$). Doses for a total of 1004 points were measured by RPLGDs and calculated with planning software in the following locations: rectum ($n = 549$), urethra ($n = 415$), vagina ($n = 25$), and perineum ($n = 15$). Compatibility (measured dose/calculated dose) was analyzed according to dosimeter location.

Results: The compatibility for all dosimeters was 0.98 ± 0.23, stratified by location: rectum, 0.99 ± 0.20; urethra, 0.96 ± 0.26; vagina, 0.91 ± 0.08; and perineum, 1.25 ± 0.32.

Conclusions: Deviations between measured and calculated doses for the rectum and urethra were greater than 20%, which is attributable to the independent movements of these organs and the applicators. Missing corrections for inhomogeneity are responsible for the 9% negative shift near the vaginal cylinder (specific gravity = 1.24), whereas neglect of transit dose contributes to the 25% positive shift in the perineal dose. Dose deviation of >20% for nontarget organs should be taken into account in the planning process. Further development of planning software and a real-time dosimetry system are necessary to use the current findings and to achieve adaptive dose delivery. © 2008 Elsevier Inc.

Radiotherapy, *In vivo* dosimetry, Radiophotoluminescence glass dosimeter, Brachytherapy, High dose rate.

INTRODUCTION

Contemporary planning software for high-dose-rate (HDR) brachytherapy enables radiation oncology teams to determine conformal dose distribution to the target while avoiding excessive doses to critical organs (1–4); however, reproducibility of planned doses in interstitial brachytherapy has not been well recognized. Few studies have investigated *in vivo* dosimetry for interstitial brachytherapy; previous studies have dealt with small numbers of patients (≤10 patients, to the best of our knowledge) and have been limited to the use of thermoluminescence dosimeters (TLD), the use of which involves complex handling processes (5–9).

A radiophotoluminescence glass dosimeter (RPLGD) was developed in the 1950s and has subsequently been used for radiotherapeutic dosimetry at a small number of centers (10–14). Irradiation of silver-activated phosphate glass converts silver ions to stable luminescent centers; when exposed to ultraviolet light, the luminescent centers produce fluorescence in proportion to the absorbed radiation dose. RPLGDs possess ideal properties for *in vivo* dosimetry, including small

Reprint requests to: Takayuki Nose, M.D., Department of Radiation Oncology, The Cancer Institute Hospital of the Japanese Foundation for Cancer Research, 3-10-6 Ariake, Koto-Ku, Tokyo 135-8550, Japan. Tel: (+81) 3-3520-0111; Fax: (+81) 3 3570 0343; E-mail: takayuki.nose@jfcr.or.jp

Conflict of interest: none.

Acknowledgments—The authors are grateful to Dr. Teizou Tomaru (Chiyoda Technol) and Mr. Tatsuya Ishikawa (Asahi Techno Glass) for their valued advice concerning radiation physics. This study was supported in part by a Grant-in-Aid for Scientific Research (C) from the Japan Society for the Promotion of Science (18591397). This study was presented at the 12th International Brachytherapy Conference, June 20–23, 2007, in Rome, Italy.

Received March 3, 2007, and in revised form Sept 19, 2007. Accepted for publication Sept 21, 2007.

size, ruggedness, nontoxicity, photon-energy independence over the energy range >0.2–0.3 MeV, high sensitivity, good reproducibility, and repeat readability until annealing of the detectors. Advances in technology (10–15) have helped to overcome initial shortcomings in the method, such as energy dependence in the low-energy range of <0.1 MeV, susceptibility to spurious readings with surface contamination, and the necessity for complex handling and cleaning processes. Newly developed RPLGDs (Dose Ace, Chiyoda Technol, Tokyo, Japan) were used in the current study (10–12). In our previous study, using RPLGD, we performed the largest *in vivo* dosimetry study examined at that time by measuring 83 points in 61 head and neck cancer patients (12). In the current study, we investigate the reproducibility of pelvic interstitial brachytherapy by measuring 1004 points in 66 pelvic malignancy patients. On the basis of the results, we investigated the limits of available planning software and a potential solution for precise dose delivery.

PATIENTS AND METHODS

Patients

Sixty-six patients with pelvic malignancy underwent HDR interstitial brachytherapy (HDRIB) with RPLGD at Osaka Medical Center (OMC) between 2000 and 2003. Patient characteristics are presented in Table 1, The median follow-up period was 30 months (range, 1–58 months). Forty-three patients displayed nonrecurrent disease, and 23 patients displayed recurrent disease following surgery ($n = 11$), radiation ($n = 4$), or both ($n = 8$). All patients were informed of the study purposes and possible consequences. Written informed consent was obtained before participation.

Radiophotoluminescence glass dosimeter

The RPLGD (Dose Ace) is more robust than TLDs and is composed of uniform glass with an effective atomic number of 12.039; it contains 11.00% Na, 31.55% P, 51.16% O, 6.12% Al, and 0.17% Ag by weight (10). The element is 1.5 mm in diameter and 8.5 mm in length, which is similar to commercially available TLD rods. The sensitive volume is located centrally and measures 1.5 mm in diameter and 6.0 mm in length; a portion 1.5 mm in diameter and 1.25 mm in length at each end is not used for dosimetry. The dispersion of response among dosimeters is small (coefficient of variation [ratio of the standard deviation to the mean] = 0.82%), and the reproducibility of repeat measurements by a single element is excellent (coefficient of variation = 0.29%), being superior to that of commercially available TLDs (10). Moreover, handling of the RPLGD is easier than for TLDs. A reader (FGD-1000, Chiyoda Technol, Tokyo, Japan) stimulates the RPLGD using a pulsed ultraviolet laser. Differences in fluorescence decay time between surface contamination (0.3 μs) and radiophotoluminescence (3 μs) enable discrimination between signal arising from contamination with finger grease or mucus from that due to absorbed radiation dose (10, 15, 16); thus, the new detector can be easily inserted and removed manually into and out of vectors and can be applied to regions in close contact with mucus because it does not require the complex cleaning processes necessary for TLDs and early RPLGDs. The reader repeats measurements 10–50 times within a few seconds and averages the values to reduce random errors. The quantity of radiophotoluminescence of a RPLGD is compared with that of a standard detector within the reader that has been irradiated with a known dose; the readout is expressed in Gy. Readout range is 10 μGy to 10 Gy, extendable to 500 Gy with optional settings. These new capabilities, coupled with the inherent properties of RPLGDs, mean that the new dosimeter can be easily applied to *in vivo* dosimetry studies. A preheat process at 70°C for 30 min and a cooling process to room temperature are necessary before each reading for which immediate reading after irradiation cannot be achieved. The details of individual correction factors derived using 4 MV X-rays have previously been described (12). For the 100 RPLGDs used in the current study, the coefficient of variation was 1.41% for dispersion among detectors, and the mean coefficient of variation for three-time repeat measurement was 1.29%. The linear dose response for RPLGD ($r = 1.000$, $p < 0.01$) for 1 to 136 Gy has been confirmed in our previous study (12).

Table 1. Patient characteristics

Age	Median 64 (35–81)
Sex	Male 30, female 36
Follow-up	Median 30 (1~58) months
Primary site	
Prostate	26
Gynecological	35 (previously irradiated 11)
Miscellaneous	5 (previously irradiated 1)
Total	66

RPLGD Vectors

Three types of vectors were developed for this study. Type 1 is a single "RPLGD complex", which was loaded to a 1.5-mm-deep slot carved on the upper part of the vaginal cylinder or on the perineal side of the template and was covered with gum paint (Fig. 1a); the RPLGD was located centrally, with a ø1-mm lead ball placed at each end as a radio-opaque marker. A 1-mm-long urethane spacer was placed between the RPLGD and each lead ball to avoid scratching. The Type 2 vector, used for the urethra, comprised a train of 10 "RPLGD complexes" loaded in a ø2-mm Teflon tube (Figs. 1b and 1c). The Type 3 vector, dedicated to the rectum, used a ø4-mm Teflon tube into which a train of 10 "encapsulated RPLGD complexes" was loaded manually; each RPLGD was contained in a plastic capsule to avoid excessive contamination by mucus (Fig. 1d). Three nylon threads were sutured to each end and to the midportion of the vector for fixation to the rectum.

Implantation

Implantation was performed in a lithotomy position under general and epidural anesthesia with or without spinal anesthesia. Before implantation, the Type 3 vector was sutured to the anterior rectal wall through a rigid rectoscope (Figs. 2a, 2b, and 2c). The entire vector length was kept in contact with the mucosa using at least three stitches; additional sutures were used if the vector was not in full contact with the mucosa. A median of 18 metal needles (range, 5–29) were implanted using a perineal template. Implant geometry was preplanned to cover the clinical target volume (CTV) with 85% basal dose isodose surface (BDIS) following the extrapolated Paris System to more than two-plane implants (17). Needle placement was guided by palpation and transrectal/vaginal ultrasound. For female patients, the vaginal cylinder was attached perpendicular to the template (Figs. 2a and 2b). The vaginal cylinder and metal needles were fixed to the template using screws and a template cap such that they were unified as a group and could only move

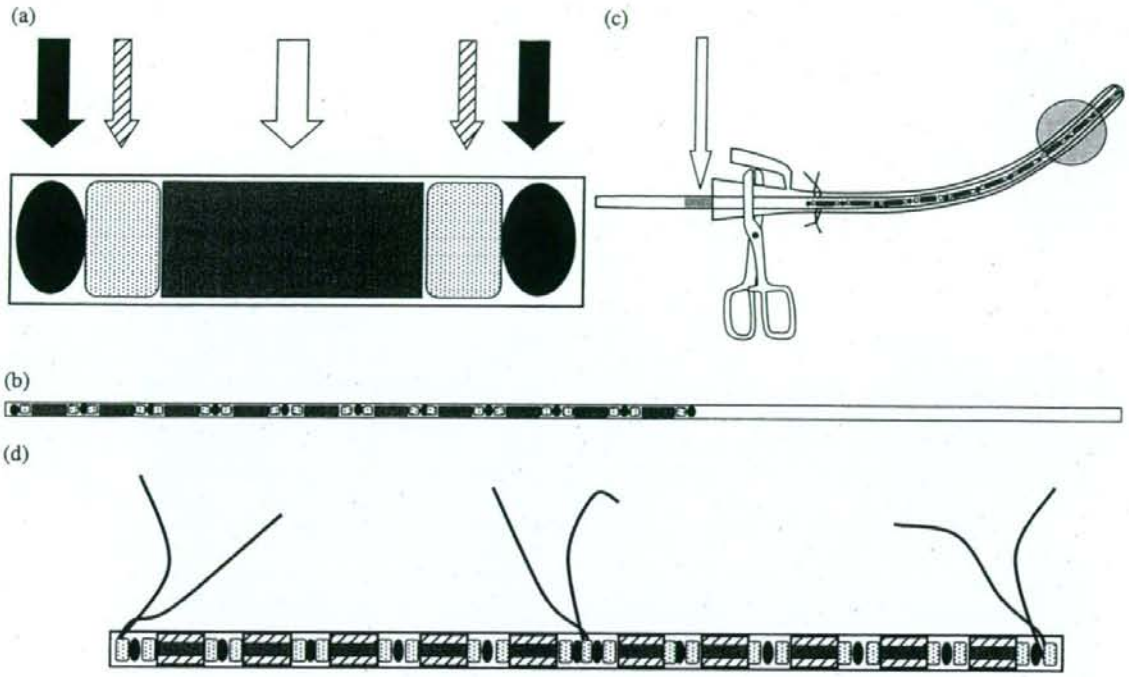

Fig. 1. (a) The Type 1 vector consists of a 1.5–mm-deep slot, carved on a vaginal cylinder or on a template; this houses an radiophotoluminescence glass dosimeter (RPLGD) complex, which consists of an RPLGD (white arrow) located centrally, a ø1 mm lead ball (black arrows) placed at each end, and 1-mm spacers (striped arrows) between the RPLGD and the lead balls. (b) The Type 2 vector, dedicated to the urethra; the ø2 mm Teflon tube contains 10 RPLGD complexes. (c) The Type 2 vector is inserted into the balloon catheter until the vector top touches the proximal catheter end at simulation and at each irradiation session. The vector and the catheter are clamped together with forceps near the distal catheter end. The point where the vector surface crosses the distal end of the catheter is marked using a felt-tip pen (arrow). (d) The Type 3 vector, dedicated to the rectum, is shown; the ø4-mm Teflon tube contains 10 encapsulated RPLGD complexes, with each RPLGD housed in a plastic capsule. The three nylon threads sutured to each end and the midportion of the vector enable fixation of the vector to the rectum.

synchronously. For most female patients, tumor extent involved the vaginal wall such that vaginal wall dosimetry represented tumor dose. The template was sutured to the perineum such that the Type 1 RPLGD was in contact with the skin (Figs. 2a and 2b). Template dosimetry represented perineal skin dose. A balloon catheter was sutured to the urethral orifice after early experiences with the prostate implant and anterior vaginal implant in particular; the needle tips had collapsed the balloon and caused migration of the catheter from the original position. A total of 1142 points were measured by RPLGDs in the following locations: anterior wall of the rectum, $n = 599$; urethra, $n = 482$; vaginal cylinder, $n = 28$; perineal template, $n = 33$. Doses were measured by RPLGDs and were also calculated on a planning computer (CadplanBT 1.1, Varian TEM, Crawley, United Kingdom). Of the 1142 points, 58 points (5.1%) were not identified by X-ray films, and dose calculation was not obtainable; therefore, both measured and calculated doses were available for 1084 points.

Simulation, planning, and irradiation

At simulation, the Type 2 vector was inserted into the balloon catheter until the vector top touched the proximal end of the catheter (Fig. 1c). Both the vector and the catheter were clamped together with forceps near the distal end of the catheter. The point where the vector surface crossed the distal end of the catheter was marked with a felt-tip pen to enable reproducible loading at each session. A dummy source was loaded into each applicator. A pair of radiographs was taken; the couch was then rotated 90°, and CT was performed at 5-mm intervals; all measured doses were therefore contaminated by simulation radiation. CadplanBT 1.1 was used for treatment planning. The geometry of the applicators was reconstructed from the radiographs before the superimposition of CT data. The central plane and basal dose points were determined according to the extrapolated Paris System (17, 18). An arbitrary isodose surface (median, 82% BDIS; range, 70%–98% BDIS) that covered the CTV was chosen for dose prescription. HDRIB schedules are described in Table 2; rectal and urethral doses represent constraints for dose prescription. For patients not previously irradiated, calculated rectal and urethral doses were set to a below-ceiling dose that was determined on the basis of clinical experiences of HDRIB at Osaka University and related hospitals (Table 2). For the 12 reirradiated patients, the previous radiotherapy consisted of 30-Gy whole pelvis (range, 0–50 Gy) and 10-Gy central-shielded field (range, 0–28 Gy) combined with 30-Gy HDR intracavitary brachytherapy ($n = 6$, range, 15–30 Gy) or 36 Gy HDRIB ($n = 1$). It was impractical to set a ceiling dose for these patients, and doses for

the rectum/urethra were modified to as low as possible. The maximum diameter of double the prescription isodose surface (hyperdose sleeve) was another concern related to morbidity. The Paris System recommends keeping this diameter ≤8–10 mm (18). If the diameter exceeded 8 mm, the dose distribution was modified by manually changing dwell times. When these three conditions (CTV coverage, rectal/urethral dose, hyperdose sleeve ≤8 mm) could not be achieved simultaneously, the plan was compromised at the cost of rectal/urethral dose, hyperdose sleeve, or both. For each RPLGD, three points (the midpoint and both ends of the readout part) were reconstructed. Doses were calculated for the three points, and the averaged value was regarded as the calculated dose for the particular RPLGD. The anatomic location of the RPLGD was classified as "anterior wall of the rectum"; "urethra (male/female)"; "vaginal wall," measured at the vaginal cylinder surface; and "perineal skin," measured at the template surface facing the perineum. Irradiation was performed using Varisource (Varian TEM). Source strength was determined following each purchase using a well-type chamber. The mean deviation from the supplier's value was only 0.08 ± 0.83% (range, –1.04 to 1.60%). HDRIB was delivered twice a day with an interval of at least 6 h. Before each session, the Type 2 vector was inserted into the balloon catheter to the depth of the felt-tip pen marker crossing the catheter (Fig. 1c).

(a)

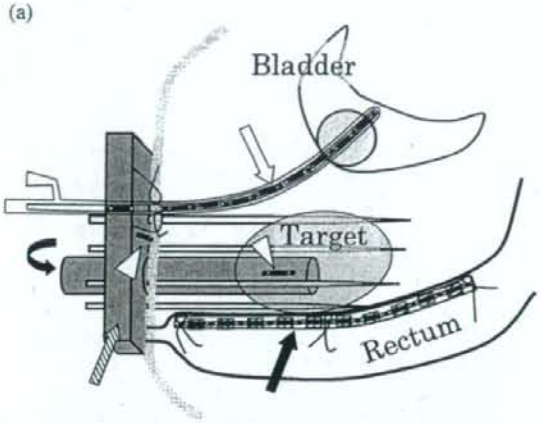

(b)

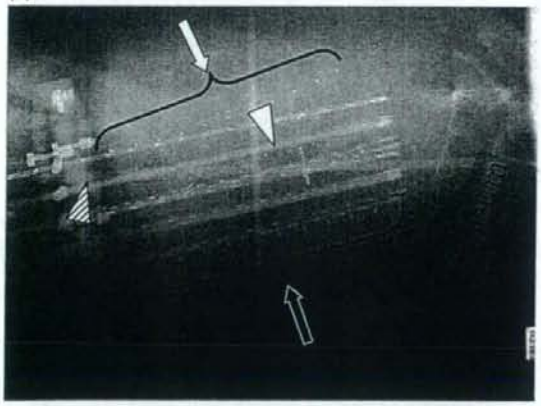

(c)

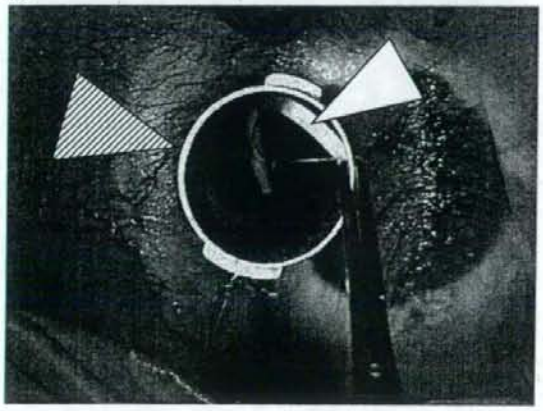

Absorbed simulation X-ray

Absorbed dose from the simulation was assessed in one prostate cancer patient using a Type 2 vector in the urethra. During a routine simulation, 10 RPLGDs in the urethra were exposed to 120 KV X-rays (mean effective energy ≈ 40 KeV) for a pair of radiographs and a 20-cm CT at 5-mm intervals. The readout value was corrected by both calibration factors for each RPLGD, as obtained for 4-MV photons, and by a relative correction factor of 3.8 for 40 KeV (Fig. A, 9.4 in ref. 16).

Statistics

Statistical analyses were performed using SPSS 8.0 software (Chicago, IL). The Mann-Whitney *U* test was used for nonparametric comparisons (19). Kaplan-Meier methods were used for analyses of local control (20).

RESULTS

Clinical results

There were no unexpected events attributable to the use of RPLGDs. Moreover, the location of anterior rectal wall that is not visible on CT was easily found, and the corresponding dose was calculated. In all patients, the use of RPLGD was well tolerated. The local control ratio was 87% with a median follow-up of 30 months. Late sequelae were graded as G0 in 38 patients, G1 in 6 patients, G2 in 5 patients, G3 in 7 patients, and not specified in 10 patients.

Fig. 2. (a) Schema of the current study. Application of two Type 1 radiophotoluminescence glass dosimeter (RPLGD) complexes: one on the template, the other on the vaginal cylinder (arrowheads); one Type 2 vector in a balloon catheter (white arrow); and one Type 3 vector on the anterior rectal wall (black arrow) for a female patient. The striped arrow indicates the perineal template and vaginal cylinder (curved arrow). (b) A radiograph from the study shows the application positions of the following vectors: Type 1 vectors on the template (striped arrowhead) and on the vaginal cylinder (white arrowhead); Type 2 vector in a balloon catheter (white arrow); and Type 3 vector on the anterior rectal wall (black arrow) of a female patient. (c) A Type 3 vector (white arrowhead) is sutured to the anterior rectal wall through a rigid rectoscope (striped arrowhead).

Table 2. HDRIB schedule

	HDRIB	EXRT	Ceiling dose for rectum	Ceiling dose for urethra
HDRIB alone (n = 45)				
Previously nonirradiated (n = 33)	54 Gy/9 fr/5 d	-	42 Gy/9 fr/5 d	76 Gy/9 fr/5 d
Previously irradiated (n = 12)	48 Gy/8 fr/4 d	-	Not specified	Not specified
HDRIB+EXRT (n = 21)				
Previously nonirradiated (n = 21)	30 Gy/5 fr/3 d	WP 30 Gy + CS 20 Gy	24 Gy/5fr/3 d	58 Gy/5 fr/3 d

Abbreviations: HDRIB = high-dose-rate interstitial brachytherapy; EXRT = external radiotherapy; fr = fraction; WP = whole pelvis field; CS = central-shielded field.

Absorbed simulation X-ray by RPLGDs

The median measured dose of all 1084 points was 17.19 Gy (range, 0.41–88.73 Gy). The median absorbed simulation dose for the 10 RPLGDs was 0.048 Gy (range, 0.043–0.054 Gy), corresponding to 1.06% (0.048 Gy × 3.8 / 17.19 Gy; range, 0.21% [0.048 Gy × 3.8 / 88.73 Gy] to 44.49% [0.048 Gy × 3.8 / 0.41 Gy]) of the median absorbed dose. Setting the threshold for the simulation dose at 5% of the total absorbed dose, 3.65 Gy (0.048 Gy × 3.8 / 5%) was the minimum total measured dose required. Doses for 80 points (rectum, n = 30; urethra, n = 41; vagina, n = 1; perineum, n = 8) were <3.65 Gy; these values were eliminated from further analyses.

Results of 1004 RPLGDs

The remaining 1004 points (≥3.65 Gy), comprised of rectum, n = 549; urethra, n = 415; vaginal wall, n = 25; and perineal skin, n = 15 were used for further analyses. For the 1004 dosimeters, the median measured and calculated doses were 18.59 Gy (range, 3.65–88.73 Gy) and 19.94 Gy (range, 2.42–94.68 Gy), respectively. The compatibility ratio of the measured and calculated doses was 0.98 ± 0.23. Measured doses, calculated doses, and compatibility according to location are displayed in Table 3. The frequencies of compatibility according to location are displayed in Figs. 5a–5e.

Dose for the rectum

For the 549 dosimeters, the median measured and calculated doses were 17.64 Gy (range, 3.68–64.64 Gy) and 18.32 Gy (range, 3.19–75.70 Gy), respectively. The compatibility ratio of the measured and calculated doses was 0.99 ± 0.20 (Fig. 3a).

Dose for the urethra (female and male)

For the 415 dosimeters, the median measured and calculated doses were 20.47 Gy (range, 3.72–88.73 Gy) and 21.65 Gy (range, 2.58–78.84 Gy), respectively. The compatibility ratio of the measured and calculated doses was 0.96 ± 0.26.

Dose for the male urethra

For the 181 dosimeters, the median measured and calculated doses were 28.31 Gy (range, 4.07–88.73 Gy) and 36.73 Gy (range, 3.35–78.84 Gy), respectively. The compatibility ratio of the measured and calculated doses was 0.90 ± 0.30 (Fig. 3b). The ratio for the male urethra was significantly different from that for the female urethra (p <0.01). Even with stitches to the urethral orifice in males, if the balloon was ruptured by the needle tips, the balloon catheter could migrate, depending on penis direction and length. A 10% negative shifted distribution suggests slipping of the original position.

Dose for the female urethra

For the 234 dosimeters, the median measured and calculated doses were 17.51 Gy (range, 3.72–71.69 Gy) and 18.16 Gy (range, 2.58–73.03 Gy), respectively. The compatibility ratio of the measured and calculated doses was 1.01 ± 0.20 (Fig. 3c).

Dose for the vaginal wall

For the 25 dosimeters, the median measured and calculated doses were 38.79 Gy (range, 9.51–82.42 Gy) and 42.98 Gy (range, 9.04–94.68 Gy), respectively. The compatibility ratio of the measured and calculated doses was 0.91 ± 0.08 (Fig. 3d).

Table 3. Measured dose, calculated dose, and compatibility according to locations for the 1004 points

Region	Measured dose	Calculated dose	Compatibility ratio*
Anterior wall of the rectum (n = 549)	17.6 Gy (3.7–64.6 Gy)	18.3 Gy (3.2–75.7 Gy)	0.99 ± 0.20
Urethra (n = 415)	20.5 Gy (3.7 Gy-88.7 Gy)	21.7 Gy (2.6 Gy-78.8 Gy)	0.96 ± 0.26
Male urethra (n = 181)	28.3 Gy (4.1 Gy-88.7 Gy)	36.7 Gy (3.4 Gy-78.8 Gy)	0.90 ± 0.30
Female urethra (n = 234)	17.5 Gy (3.7 Gy-71.7 Gy)	18.2 Gy (2.6–73.0 Gy)	1.01 ± 0.20
Vaginal wall (n = 25)	38.8 Gy (9.5 Gy-82.4 Gy)	43.0 Gy (9.0–94.7 Gy)	0.91 ± 0.08
Perineal skin (n = 15)	6.9 Gy (3.7 Gy-59.6 Gy)	6.3 Gy (2.4–61.6 Gy)	1.25 ± 0.32
Total (n = 1004)	18.6 Gy (3.7 Gy-88.7Gy)	19.9 Gy (2.4–94.7 Gy)	0.98 ± 0.23

* Compatibility ratio = measured dose/calculated dose.

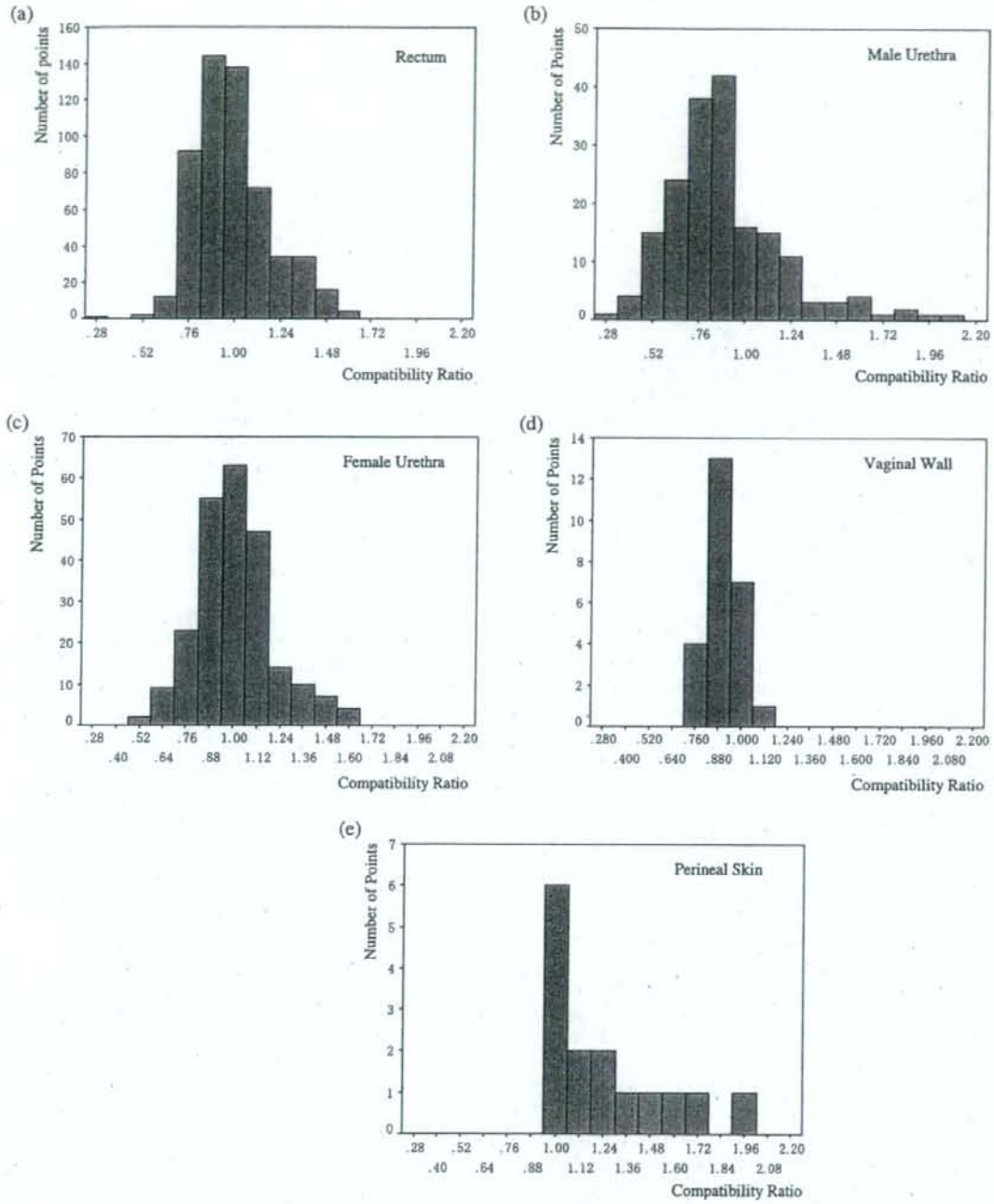

Fig. 3. (a) Frequency of compatibility ratio for radiophotoluminescence glass dosimeter (RPLGD) for the rectum. Abscissa: ratio of measured dose/calculated dose. Ordinate: number of points for RPLGDs. Distribution approximates Gaussian, with mean compatibility of 0.99 ± 0.20. (b) Frequency of compatibility ratio for RPLGD for the male urethra. Abscissa: ratio of measured dose/calculated dose. Ordinate: number of RPLGDs. Distribution is positive-skewed and negatively shifted, with mean compatibility of 0.90 ± 0.30. (c) Frequency of compatibility ratio for RPLGD for the female urethra. Abscissa: ratio of measured dose/calculated dose. Ordinate: number of RPLGDs. Distribution approximates Gaussian, with mean compatibility of 1.01 ± 0.20. (d) Frequency of compatibility ratio for RPLGD for the vaginal wall. Abscissa: ratio of measured dose/calculated dose. Ordinate: number of points for RPLGDs. Distribution is negatively shifted steep Gaussian, with mean compatibility of 0.91 ± 0.08. (e) Frequency of compatibility ratio for RPLGD for the perineum. Abscissa: ratio of measured dose/calculated dose. Ordinate: number of RPLGDs. Distribution is positive-skewed and with mean compatibility of 1.25 ± 0.32.

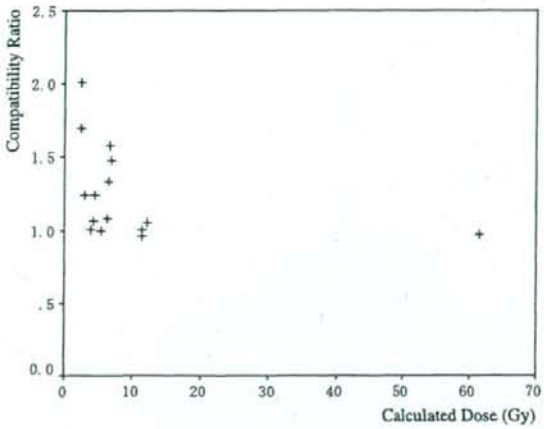

Fig. 4. Correlation between compatibility ratio (ordinate; measured dose/calculated dose) and the calculated dose (abscissa) for perineal skin.

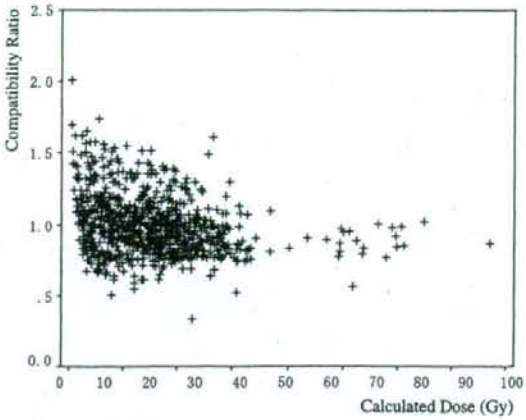

Fig. 5. Correlation between compatibility ratio (ordinate; measured dose/calculated dose) and the calculated dose (abscissa) for 823 points (male urethra excluded).

Dose for the perineal skin

For the 15 dosimeters, the median measured and calculated doses were 6.85 Gy (range, 3.65–59.62 Gy) and 6.33 Gy (range, 2.42–61.64 Gy), respectively. The compatibility ratio of the measured and calculated doses was 1.25 ± 0.32 (Fig. 3e). Transit dose plays an important role in positive discrepancy of the measured dose and its impact is known to depend on the calculated dose (21). Compatibility ratio according to calculated dose is displayed in Fig. 4.

DISCUSSION

In vivo dosimetry studies for interstitial brachytherapy have previously dealt only with small numbers of patients, except for pioneering work using RPLGDs at the Veterans Administration Hospital in New York in the 1950s and 1960s (5–9, 13). To the best of our knowledge, this is the largest *in vivo* dosimetry study conducted for interstitial brachytherapy. The simple handling of RPLGDs facilitates their routine use in clinical situations; in addition, their linearity and reproducibility are better than those of the TLDs used previously (5–9). Measured doses in this study were contaminated by simulation X-rays; data with excessive contamination were excluded by setting a threshold for measured doses.

For male urethral measurements, suturing of the catheter to the urethral orifice did not eliminate the migration of dosimeters that prevents precise data from being obtained. For female urethral measurements, this technique eliminated migration. The frequency for compatibility of measured and calculated doses displayed a wide Gaussian distribution, with mean 1.01 ± 0.20. For the rectum, compatibility displayed a similar Gaussian distribution (0.99 ± 0.20). These deviations (±20%) are attributable to the movements for these organs independent of movement for the target, and hence for the applicators. In our previous *in vivo* dosimetry study for 61 head and neck brachytherapy patients, the compatibility for nontarget organs (the submandibular skin and the mandible) displayed a wider Gaussian distribution, with mean 1.06 ± 0.32 (12). The movement of nontarget organs relative to the applicators is less in the pelvic region (where target organs and applicators do not move voluntarily) than in the head and neck region (where target organs move under the control of voluntary muscles). For nontarget organs in the pelvic region, actual absorbed doses can be 20% greater than calculated doses, compared with 32% in the head and neck region. Lead shielding is an effective protection that halves the absorbed dose to the nontarget organs in the region of the head and neck (4); however, shielding is impractical for the rectum and urethra during interstitial brachytherapy. Actual dose monitoring for organs at risk is feasible by employing an alternative real-time dosimeter such as MOSFET (22). If excessive dose is detected, the initial planning can be adapted for subsequent sessions.

For the target (vaginal wall), compatibility displayed a narrow Gaussian distribution (0.91 ± 0.08). This 8% deviation is the smallest among all the locations and is similar to the 10% deviation (0.95 ± 0.10) observed for the head and neck target in our previous study (12). Movement of the target is synchronized with the applicators, provided that the applicators are implanted in the target, irrespective of the target type and movement pattern (pelvis, nonvoluntary movement by surrounding organ volumes; head and neck, voluntary movement). The 9% negative shift is attributable to the lack of inhomogeneity correction in the software for the vaginal cylinder, which has a density of 1.24. The acceptable criteria for brachytherapy, as stated by the Radiological Physics Center, is 15% (23), which is achievable using inhomogeneity correction. Use of a real-time dosimeter is desirable to achieve more precise delivery of the planned dose.

The transit dose affects all the measured doses to some degree. The importance of the transit dose depends on calculated dose (21). As shown in Fig. 4, the calculated dose seems to affect the compatibility ratio for the perineal skin.

The compatibility ratio approaches unity as the calculated dose increases, especially for >10 Gy. For 823 points (excluding male urethral points), 294 points were to receive calculated dose <10 Gy, and the compatibility ratio was 1.09 ± 0.25, whereas 529 points were to receive calculated dose ≥10 Gy, and the compatibility ratio was 0.97 ± 0.18 ($p < 0.001$) (Fig. 5). Transit dose should be incorporated in points with calculated dose <10 Gy, although the clinical impact of these low doses remains unclear.

In conclusion, the compatibility ratio of the measured and calculated doses for the target displayed a small deviation (8%) caused by synchronized movement with the applicators, and a 9% negative shift attributable to the cylinder material. The addition of inhomogeneity correction to the planning software would enable the acceptable criteria for the target of brachytherapy (15%) to be easily achieved. The transit dose should be incorporated into points with a calculated dose of <10 Gy. Measured doses for organs at risk displayed as much as 20% deviation from the planned doses because of involuntary movements. The next step to using these findings will be to establish an adaptive dose delivery system using a real-time dosimeter.

REFERENCES

1. Lachance B, Béliveau-Nadeau D, Lessard É, *et al.* Early clinical experience with anatomy-based inverse planning dose optimization for high-dose-rate boost of the prostate. *Int J Radiat Oncol Biol Phys* 2002;54:86–100.
2. Sumida I, Shiomi H, Yoshioka Y, *et al.* Optimization of dose distribution for HDR brachytherapy of the prostate using attraction-repulsion model. *Int J Radiat Oncol Biol Phys* 2006;64: 643–649.
3. Nose T, Peiffert D, Lapeyre M, *et al.* Clinical target volume-based dose specification for interstitial brachytherapy: Minimum target dose comparison with classical implant system. *J Brachyther Int* 2001;17:345–353.
4. Nose T, Koizumi M, Nishiyama K. High-dose-rate interstitial brachytherapy for oropharyngeal carcinoma: Results of 83 lesions in 82 patients. *Int J Radiat Oncol Biol Phys* 2004;59: 983–991.
5. Mangold CA, Rijnders A, Georg D, *et al.* Quality control in interstitial brachytherapy of the breast using pulsed dose rate: Treatment planning and dose delivery with an Ir-192 afterloading system. *Radiother Oncol* 2001;58:43–51.
6. Brezovich IA, Duan J, Pareek PN, *et al.* In vivo urethral dose measurements: A method to verify high dose rate prostate treatments. *Med Phys* 2000;27:2297–2301.
7. Hamers HP, Johansson KA, Venselaar JLM, *et al.* In vivo dosimetry with TLD in conservative treatment of breast cancer patients treated with the EORTC protocol 22881. *Acta Oncol* 1993;32:435–443.
8. Anagnostopoulos G, Baltas D, Geretschlaeger A, *et al.* In vivo thermoluminescence dosimetry dose verification of transperineal ^{192}Ir high-dose-rate brachytherapy using CT-based planning for the treatment of prostate cancer. *Int J Radiat Oncol Biol Phys* 2003;57:1183–1191.
9. Kälkner KM, Bengtsson E, Eriksson S, *et al.* Dosimetry of anal radiation in high-dose-rate brachytherapy for prostate cancer. *Brachytherapy* 2007;6:49–52.
10. Tsuda M. A few remarks on photoluminescence dosimetry with high energy X-rays. *Jpn J Med Phys* 2000;20:131–139.
11. Araki F, Ikegami T, Ishidoya T, *et al.* Measurements of Gamma-Knife helmet output factors using a radiophotoluminescent glass rod dosimeter and a diode detector. *Med Phys* 2003;30: 1976–1981.
12. Nose T, Koizumi M, Yoshida K, *et al. In vivo* dosimetry of high-dose-rate brachytherapy: Study on 61 head-and-neck cancer patients using radiophotoluminescence glass dosimeter. *Int J Radiat Oncol Biol Phys* 2005;61:945–953.
13. Roswit B, Malsky SJ, Reid CB, *et al.* In vivo radiation dosimetry. Review of a 12-year experience. *Radiology* 1970;97:413–424.
14. Perry JA. Luminescence phenomena. In: Perry JA, editor. RPL dosimetry. Radiophotoluminescence in health physics. Bristol, United Kingdom: IOP; 1987. p. 1–7.
15. Perry JA. Instrumentation and technique. In: Perry JA, editor. RPL dosimetry. Radiophotoluminescence in health physics. Bristol, United Kingdom: IOP; 1987. p. 141–160.
16. Japan Society of Medical Physics, editor. Standard dosimetry of absorbed dose in external beam radiotherapy (Standard Dosimetry 01). Tokyo: Tsuusyou Sangyou Kenkyu; 2002 [in Japanese].
17. Leung S. Perineal template techniques for interstitial implantation of gynecological cancers using the Paris System of dosimetry. *Int J Radiat Oncol Biol Phys* 1990;19:769–774.
18. Dutreix A, Marinello G, Wambersie A. Dosimétrie du système de Paris. In: Dutreix A, Marinello G, Wambersie A, editors. Dosimétrie en curiethérapie. Paris: Masson; 1982. p. 109–138.
19. Siegel S. In: Nonparametric statistics for the behavioral sciences. New York: McGraw-Hill; 1956.
20. Kaplan EL, Meier P. Nonparametric estimation for incomplete observation. *J Am Stat Assoc* 1958;53:457–511.
21. Thomadsen BR, Houdek PV, van der Laarse R, *et al.* Treatment planning and optimization. In: Nag S, editor. High dose rate brachytherapy: A text book. Armonk, NY: Futura; 1994. p. 79–145.
22. Cygler JE, Saoudi A, Perry G, *et al.* Feasibility study of using MOSFET detectors for in vivo dosimetry during permanent low-dose-rate prostate implants. *Radiother Oncol* 2006;80: 296–301.
23. Hanson WF, Shalek RJ, kennedy P. Dosimetry quality assurance in the U.S. from the experience of the Radiological Physics Center. In: Starkschall G, Horton J, editors. Quality assurance in radiotherapy physics. Madison, WI: Medical Physics; 1991. p. 255–282.

Int. J. Radiation Oncology Biol. Phys., Vol. 72, No. 4, pp. 1168–1173, 2008

0360-3016/08/$–see front matter

ELSEVIER

doi:10.1016/j.ijrobp.2008.02.054

CLINICAL INVESTIGATION **Brain**

INCIDENCE OF BRAIN ATROPHY AND DECLINE IN MINI-MENTAL STATE EXAMINATION SCORE AFTER WHOLE-BRAIN RADIOTHERAPY IN PATIENTS WITH BRAIN METASTASES: A PROSPECTIVE STUDY

YUTA SHIBAMOTO, M.D.,*† FUMIYA BABA, M.D.,*† KYOTA ODA, M.D.,† SHINYA HAYASHI, M.D.,† MASAKI KOKUBO, M.D.,† SHUN-ICHI ISHIHARA, M.D.,† YOSHIYUKI ITOH, M.D.,† HIROYUKI OGINO, M.D.,*† AND MASAHIKO KOIZUMI, M.D.†

*Department of Radiology, Nagoya City University Graduate School of Medical Sciences, Nagoya, Japan; and †Chubu Radiation Oncology Group, Nagoya, Japan

Purpose: To determine the incidence of brain atrophy and dementia after whole-brain radiotherapy (WBRT) in patients with brain metastases not undergoing surgery.

Methods and Materials: Eligible patients underwent WBRT to 40 Gy in 20 fractions with or without a 10-Gy boost. Brain magnetic resonance imaging or computed tomography and Mini-Mental State Examination (MMSE) were performed before and soon after radiotherapy, every 3 months for 18 months, and every 6 months thereafter. Brain atrophy was evaluated by change in cerebrospinal fluid–cranial ratio (CCR), and the atrophy index was defined as postradiation CCR divided by preradiation CCR.

Results: Of 101 patients (median age, 62 years) entering the study, 92 completed WBRT, and 45, 25, and 10 patients were assessable at 6, 12, and 18 months, respectively. Mean atrophy index was 1.24 ± 0.39 (SD) at 6 months and 1.32 ± 0.40 at 12 months, and 18% and 28% of the patients had an increase in the atrophy index by 30% or greater, respectively. No apparent decrease in mean MMSE score was observed after WBRT. Individually, MMSE scores decreased by four or more points in 11% at 6 months, 12% at 12 months, and 0% at 18 months. However, about half the decrease in MMSE scores was associated with a decrease in performance status caused by systemic disease progression.

Conclusions: Brain atrophy developed in up to 30% of patients, but it was not necessarily accompanied by MMSE score decrease. Dementia after WBRT unaccompanied by tumor recurrence was infrequent. © 2008 Elsevier Inc.

Whole-brain radiation, Brain metastasis, Brain atrophy, Dementia, Mini-Mental State Examination.

INTRODUCTION

Before the establishment of stereotactic radiosurgery (SRS), whole-brain radiotherapy (WBRT) was the golden standard of treatment for patients with brain metastases (1). Currently, patients with single or oligometastases frequently are treated with SRS, whereas those with four or more metastases are considered to be indicated for WBRT; after SRS alone, the expected probability of tumor recurrence in the unirradiated areas is very high (2, 3). Nevertheless, many patients with four or more metastases are treated by means of SRS alone without undergoing WBRT, especially in Japan (4, 5). One of the major reasons for avoiding WBRT is the fear that WBRT may cause dementia, as well as brain atrophy. However, there are no data clearly indicating the incidence of such late adverse effects of cranial irradiation, and there are only retrospective studies suggesting the occurrence of these complications (6–11). Many patients reported previously were treated with surgery and radiation (9, 10); therefore, it is unclear whether these complications are attributable solely to radiation therapy.

Brain atrophy and dementia may be related not only to surgery, but also to tumor status and chemotherapy (12, 13). To

Reprint requests to: Yuta Shibamoto, M.D., Department of Radiology, Nagoya City University Graduate School of Medical Sciences, 1 Kawasumi, Mizuho-cho, Mizuho-ku, Nagoya 467-8601, Japan. Tel: (+81) 52-853-8274; Fax: (+81) 52-852-5244; E-mail: yshiba@med.nagoya-cu.ac.jp

Presented at the 48th Annual Meeting of the American Society for Therapeutic Radiology and Oncology (ASTRO), Philadelphia, PA, November 5–9, 2006.

Conflict of interest: none.

Acknowledgments—We thank Drs. Chikao Sugie, Kana Kobayashi, Natsuo Tomita, Chisa Hashizume, and Souichiro Mori for their contribution in collecting data. Author affiliations are Department of Radiotherapy, Aizawa Hospital, Matsumoto, Japan (K.O.), Department of Radiology, Gifu University Hospital, Gifu, Japan (S.H.), Institute of Biomedical Research and Innovation, Kobe, Japan (M.K.), Department of Radiology, Nagoya University Hospital, Nagoya, Japan (S.I., Y.I.), and Faculty of Radiological Technology, Fujita Health University School of Health Sciences, Toyoake, Japan (M.K.).

Received Jan 21, 2008, and in revised form Feb 16, 2008. Accepted for publication Feb 21, 2008.

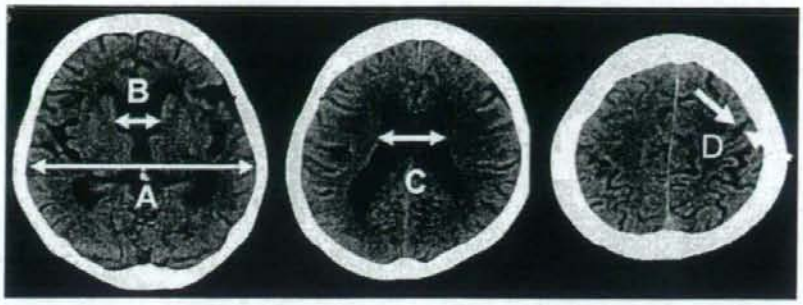

Fig. 1. Methods for calculation of cerebrospinal fluid–cranial ratio (CCR): (A) maximal distance between the internal tables of the skull, (B) minimal width of the frontal horns, (C) minimal width of bodies of the lateral ventricles, and (D) number of sulci of 3.3 mm or greater on a slice 7 cm above the orbitomeatal line. CCR is obtained by $42.66 \times B/A + 12.52 \times C/A + 0.232 \times D - 2.92$.

properly evaluate the incidence of radiation-induced brain atrophy and dementia, we considered it necessary to carry out a prospective study to exclude as much as possible the influence of other factors. In this report, we present results of a prospective study of the Chubu Radiation Oncology Group, Japan (CROG-0301), that estimated the incidence of decrease in Mini-Mental State Examination (MMSE) scores (14) and brain atrophy after WBRT in patients with brain metastases who did not undergo a neurosurgical operation or concurrent chemotherapy.

METHODS AND MATERIALS

Eligibility

Patients who met the following criteria were considered for entry: those who were judged to be indicated for treatment with WBRT alone, with no prior brain surgery, with an MMSE score of at least 21, those who were not using and would not use corticosteroids for longer than 2 weeks, and those expected to survive at least 3 months. Considering the possibility that the presence of tumors may lower the MMSE score before treatment, the lower limit of MMSE score was set at 21, but all except 1 patient had an MMSE score of 23 or higher. This study was approved by the respective institutional review boards. Informed consent was obtained from all patients.

Table 1. Characteristics of 101 patients who entered the study

Age (y)	62 (31–78)
Men/women	52/49
WHO performance status (0/1/2/3)	9/28/33/31
Primary tumor (lung/breast/bone/colon/other)	67/24/3/2/5
Tumor number (1/2/3/≥4)	7/10/15/69
Largest tumor diameter (cm)	2.0 (0.6–8.0)
MMSE score	28 (21–30)
Cerebrospinal fluid–cranial ratio	5.5 (1.5–9.8)
Imaging modality (MRI/CT)	67/34
Total radiation dose (50/40/<40 Gy)	66/26/9
No. of assessable patients at 0/3/6/9/12/15/18/24/30/36 mo	92/68/45/30/25/17/10/4/3/3

Abbreviations: WHO = World Health Organization; MMSE = Mini-Mental State Examination; MRI = magnetic resonance imaging; CT = computed tomography.

Values expressed as median (range) or number.

We intended to obtain at least 40 assessable patients at 6 months to determine the incidence of brain atrophy and MMSE score decrease with a 95% confidence interval (CI) ± 15%. Because median survival time of patients with brain metastases was usually 4–6 months (15), but patients with an expected survival time less than 3 months were excluded from entry, it was considered necessary to accrue 100 patients.

Treatment

After evaluation, patients underwent WBRT with 2-Gy daily fractions up to 40 Gy over 4 weeks by using parallel-opposing fields. The dose was prescribed at the midline. Thereafter, a boost to main tumor sites was given when possible, with 10 Gy in five fractions. Even in patients with multiple metastases, booster radiation was recommended by excluding as much normal brain tissues as possible. When radiation field reduction was considered difficult, radiotherapy was stopped at 40 Gy. Chemotherapy was prohibited until 2 weeks after completion of WBRT.

Evaluation

Before WBRT, patients underwent contrast-enhanced magnetic resonance imaging (MRI) and/or computed tomography (CT) of the brain, in addition to physical examination and MMSE. These examinations were repeated immediately after WBRT, every 3 months for 18 months, and every 6 months thereafter. For follow-up, use of the same imaging modality (*i.e.*, either MRI or CT) was mandatory. Brain atrophy was evaluated as change in cerebrospinal fluid–cranial ratio (CCR), as proposed by Nagata *et al.* (16); the method is shown in Fig. 1. Briefly, the CCR was calculated from the equation shown in the caption of Fig. 1 by measuring the maximal distance between the internal tables of the skull, minimum width of the frontal horns of the bilateral lateral ventricles, minimum width of the bodies of the bilateral lateral ventricles, and the number of widened sulci (≥3.3 mm) on a slice 7 cm above the orbitomeatal line. The atrophy index was defined as postradiation CCR divided by preradiation CCR. Differences in incidences of brain atrophy and MMSE score decrease between groups were examined by means of Fisher's exact test. The MMSE was performed by the same radiation oncologists for respective patients.

Evaluation was terminated when intracranial lesions progressed so that evaluation was considered to be influenced by disease progression or second-line treatment became necessary. Data for these patients before this point of intracranial progression were used for analysis.

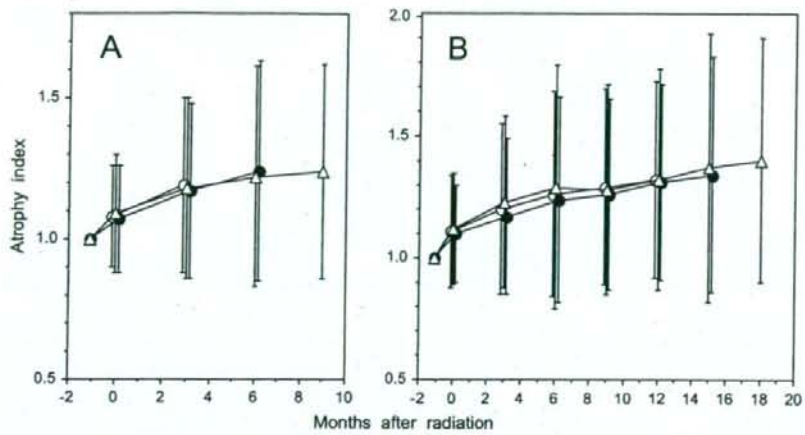

Fig. 2. Changes in mean atrophy index (A) in 68, 45, and 30 patients who were assessable for 3 (open circle), 6 (closed circle), and 9 months (open square); and (B) 25, 17, and 10 patients assessable for 12 (open circle), 15 (closed circle), and 18 months (open square), respectively. Bars represent SD.

RESULTS

Between Jan 2002 and Aug 2006, a total of 115 patients were evaluated for entry, but 14 were excluded because of low MMSE scores. Table 1 lists characteristics of the 101 patients who entered the study. Median patient age was 62 years. Ninety-three percent of patients had multiple tumors. Nine patients could not complete the planned radiotherapy because of deterioration in general conditions in 8 patients and change in treatment policy in 1 patient; therefore, post-treatment evaluation was not possible. Of the remaining 92 patients, 66 received a total dose of 50 Gy, whereas 26 underwent WBRT with 40 Gy alone.

Figure 2 shows changes in atrophy index values in groups of patients who were assessable for 3–18 months. The atrophy index tended to increase over time, although SDs were relatively large. The trend toward a mild increase in the atrophy index at completion of radiotherapy was considered to be caused by tumor response; therefore, brain atrophy was evaluated by regarding the atrophy index at completion of radiotherapy as the control level in each patient. Compared with the index at completion of radiotherapy, atrophy increased by 30% or more in 9 of 68 patients (13%; 95% CI, 5.0–21) who were assessable at 3 months, 8 of 45 patients (18%; 95% CI, 6.8–29) at 6 months, 5 of 30 patients (16%; 95% CI, 2.9–29) at 9 months, 7 of 25 patients (28%; 95% CI, 10–46) at 12 months, 5 of 17 patients (29%; 95% CI, 7.4–51) at 15 months, 3 of 10 patients (30%; 95% CI, 1.6–58) at 18 months, and 3 of 4 patients (75%; 95% CI, 33–100) at 24 months. Of 3 patients who were assessable at both 30 and 36 months, increases in atrophy index by 30% or more were seen in 2 (67%; 95% CI, 14–100). Tables 2 and 3 list incidences of 30% or greater increase in atrophy index compared with the index value immediately after radiotherapy according to patient age and radiation dose, respectively. There were no apparent differences in incidence according to age and radiation dose, although patients receiving 50 Gy (40-Gy WBRT + 10-Gy boost) tended to have a greater incidence at 9 and 12 months. Table 4 lists the incidence of 30% or greater increase in atrophy index according to pretreatment CCR. At 12 and 15 months, the incidence was greater in patients with a pretreatment CCR less than median than in those with a CCR at or greater than median.

Figure 3 shows changes in MMSE scores in groups of patients who were assessable for 3 to 18 months. Mean MMSE scores were relatively constant, and no apparent decreases were observed. However, individually, decreases in MMSE scores of four points or more were observed in 5 of 68 patients

Table 2. Incidence of 30% or greater increases in atrophy index compared with immediately after whole-brain radiation according to patient age

	Months after whole-brain radiation					
Age (y)	3	6	9	12	15	18
<60	2/32	6/27	3/16	5/13	4/9	3/5
≥60	7/36	2/18	2/14	2/12	1/8	0/5
p	0.16	0.45	1.0	0.38	0.29	0.17
<70	8/54	8/38	5/25	7/22	5/15	3/9
≥70	1/14	0/7	0/5	0/3	0/2	0/1
p	0.67	0.32	0.56	0.53	0.56	1.0

Table 3. Incidence of 30% or greater increase in atrophy index compared with immediately after whole-brain radiation according to radiation dose

	Months after whole-brain radiation					
Dose (Gy)	3	6	9	12	15	18
40 (without boost)	3/19	2/13	0/6	0/4	0/1	—
50 (with boost)	6/49	6/32	5/24	7/21	5/16	3/4
p	1.0	1.0	0.55	0.29	1.0	—

Table 4. Incidence of 30% or greater increases in atrophy index compared with immediately after whole-brain radiation according to pretreatment CCR

	Months after whole-brain radiation					
CCR	3	6	9	12	15	18
<Median	6/34	6/22	4/15	7/12	5/8	3/5
≥Median	3/34	2/23	1/15	0/13	0/9	0/5
p	0.48	0.13	0.33	0.0052	0.029	0.17

Abbreviation: CCR = cerebrospinal fluid–cranial ratio.

(7.4%; 95% CI, 1.2–14) who were assessable at 3 months, 5 of 45 patients (11%; 95% CI, 1.9–20) at 6 months, 6 of 30 patients (20%; 95% CI, 5.7–34) at 9 months, 3 of 25 patients (12%; 95% CI, 0–25) at 12 months, 1 of 17 patients (5.9%; 95% CI, 0 – 17) at 15 months, 0 of 10 patients (0%) at 18 months, 0 of 4 patients (0%) at 24 months, and 0 of 3 patients at 30 and 36 months. Table 5 lists incidences of MMSE score decrease according to patient age; there were no significant differences in incidence according to age. About half the patients with an MMSE score decrease had systemic disease progression (outside the central nervous system). There appeared to be no correlation between brain atrophy and MMSE decrease (data not shown). Seven patients received systemic chemotherapy during follow-up periods, and 1 patient had a decrease in MMSE score of four points or more at 6–12 months.

DISCUSSION

The apprehension that WBRT might cause brain atrophy and dementia seems to have grown gradually among medical oncologists and neurosurgeons. Several retrospective studies suggested it (6–11), but others reported maintenance of neurocognitive function in long-term survivors with glioma and other primary brain tumors after radiation therapy (17–20). Because retrospective studies cannot exclude the influence of other factors, such as surgery, chemotherapy, and disease progression, that can be associated with the development of brain atrophy and dementia, we conducted the present prospective study and attempted to eliminate as many of these factors as possible. As a result, we found that brain atrophy can develop in a proportion of patients, but decrease in MMSE scores was relatively infrequent. It was reported that other radiologic findings can develop after radiation to the brain, especially on MRI (21), but we used brain atrophy as an end point because it often is regarded as a late sequela of radiation linked to dementia (9). Another reason is that MRI was difficult to perform because of the long waiting time for booking in some institutions; however, brain atrophy could be evaluated easily by using CT.

We used the method of Nagata *et al.* (16) to evaluate brain atrophy. It is a simple method that can be used in multi-institutional studies, but the widths of the lateral ventricles and sulci are influenced by the mass effect of the tumors. An increase in atrophy index was found in many patients at completion of radiation therapy. This was not caused by brain atrophy, but rather tumor shrinkage. Therefore, we used atrophy index at the completion of radiotherapy as a control to evaluate posttreatment brain atrophy in individual patients. Asai *et al.* (9) reported the development of brain atrophy in 56% of patients undergoing radiation therapy. They used Nagata's method, as we did, but they defined development of brain atrophy as an atrophy index of 1.13 or higher. In our experience, measurement of CCR is not accurate enough to ensure that an atrophy index of 1.13 really represents brain atrophy. We believe an atrophy index of 1.3 is reasonable for visual recognition of brain atrophy on MRI and CT. In addition, all patients in the study of Asai *et al.* (9) had

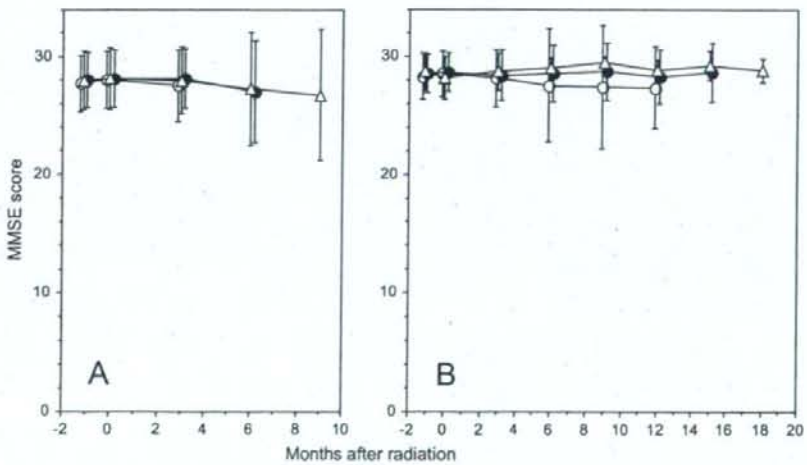

Fig. 3. Changes in mean Mini-Mental State Examination (MMSE) scores in (A) 68, 45, and 30 patients who were assessable for 3 (open circle), 6 (closed circle), and 9 months (open triangle); and (B) 25, 17, and 10 patients assessable for 12 (open circle), 15 (closed circle), and 18 months (open square), respectively. Bars represent SD.

Table 5. Incidence of decrease in Mini-Mental State Examination score of four or more points after whole-brain radiation according to patient age

	Months after whole-brain radiation					
Age (y)	3	6	9	12	15	18
<60	1/32	1/27	1/16	1/13	0/9	0/5
≥60	4/36	4/18	5/14	2/12	1/8	0/5
p	0.36	0.14	0.072	0.59	1.0	—
<70	4/54	4/38	4/25	3/22	1/15	0/9
≥70	1/14	1/7	2/5	0/3	0/2	0/1
p	1.0	1.0	0.55	1.0	1.0	—

undergone brain surgery. They reported that no brain atrophy was found after brain surgery alone, but it is not known whether surgery can be an additive factor in the development of brain atrophy when combined with radiation. In our study, excluding the influence of brain surgery, we found brain atrophy in up to 30% of patients at 6–18 months. However, about 40–50% of patients maintained an atrophy index of around 1 during these periods. We could not prove an association between the incidence of atrophy and patient age or use of the 10-Gy boost. Meanwhile, patients with a pretreatment CCR less than the median value had a greater incidence of increase in the atrophy index. This is in contrast to findings reported by Nieder *et al.* (22) showing that patients with preexisting atrophy had a greater risk of continuous deterioration. One reason for the finding in the present study may be that the index is likely to increase when the denominator (pretreatment CCR) is small.

The MMSE alone is considered to be an insensitive method to evaluate higher brain dysfunction, and it now seems clear that the combination of various neurologic tests is necessary to evaluate more subtle cognitive dysfunction (23). Therefore, the aim of the present study is to detect apparent dementia. In a prospective study comparing WBRT plus SRS and SRS alone, Aoyama *et al.* (24) evaluated changes in MMSE scores in a proportion of patients. They found that although there was no significant difference in change in MMSE scores after treatment between the two groups, the scores tended to decrease, especially after WBRT plus SRS. However, they did not clearly differentiate between disease progression–induced deterioration and treatment-related decrease. In the present study, mean MMSE score did not decrease on the whole, and proportions of patients with an MMSE score decrease of four points or more were only 11% at 6 months, 12% at 1 year, and 0% at 18 months. We excluded patients with intracranial progressive disease from further evaluation, but we did not exclude patients with systemic disease progression. As a consequence, about half the patients with an MMSE score decrease had systemic progressive disease and a decrease in performance status; thus, purely radiation-induced decrease appeared to be still less frequent. In the present study, only brain atrophy was evaluated by using MRI and CT, and there appeared to be no correlation between brain atrophy and MMSE score decrease. In additional investigations, we plan to evaluate MRI findings that may characterize patients with an MMSE score decrease.

Radiation dose per fraction may influence the occurrence of late morbidity for radiation therapy. It is well-known that central nervous system tissues have low α/β ratios and therefore are susceptible to greater doses per fraction (25). In WBRT for brain metastases, 10 fractions of 3 Gy commonly are used, but we did not use the 3-Gy/d dose in this study in the belief that a 2-Gy/d fraction is better than a 3-Gy fraction in terms of preventing late adverse effects in long-term survivors. Most previous studies reporting deterioration in neurocognitive function used 3-Gy or even higher doses per fraction (6–8, 26). In addition, 10 fractions of 3 Gy given for prophylactic cranial irradiation in patients with small-cell lung cancer are considered to be more likely to produce neurotoxicity than 2- or 2.5-Gy/d fractions (26–29). In a Radiation Therapy Oncology Group study using 10 fractions of 3 Gy for brain metastases, 81%, 66%, and 57% of patients maintained an MMSE score higher than 23 at 6, 12, and 18 months, respectively (30). Although the biologically effective dose for 10 fractions of 3 Gy is less than that for 20 fractions of 2 Gy assuming an α/β ratio of 1–4 Gy, the incidence appeared greater than that observed in the present study. Thus, use of a 2-Gy/d fraction might have contributed to the favorable effects on neurocognitive function observed in the present study. Of course, we use 3-Gy fractions for palliative cases and patients with a short expected survival time, but we will continue to use the 2-Gy fraction for patients expected to survive longer than 6 months.

In summary, the present study shows that brain atrophy can develop after WBRT in a certain proportion of patients (up to 30%), but a decrease in MMSE scores was less frequent. Avoiding WBRT for the reason that it causes dementia appears to be a groundless idea in patients with metastatic brain tumors. The WBRT with or without stereotactic boosts should be a reasonable treatment for patients with multiple brain metastases.

REFERENCES

1. Khuntia D, Brown P, Li J, *et al.* Whole-brain radiotherapy in the management of brain metastasis. *J Clin Oncol* 2006;24: 1295–1304.
2. Sneed PK, Lamborn KR, Forstner J, *et al.* Radiosurgery for brain metastases: Is whole brain radiotherapy necessary? *Int J Radiat Oncol Biol Phys* 1999;43:549–558.
3. Serizawa T, Higuchi Y, Ono J, *et al.* Gamma knife surgery for metastatic brain tumors without prophylactic whole-brain radiotherapy: Results in 1000 consecutive cases. *J Neurosurg* 2006; 105(Suppl.):S86–S90.
4. Yamamoto M, Ide M, Nishio S, *et al.* Gamma knife radiosurgery for numerous brain metastases: Is this a safe treatment? *Int J Radiat Oncol Biol Phys* 2002;53: 1279–1283.
5. Amendola BE, Wolf A, Coy S, *et al.* Radiosurgery as palliation for brain metastases: A retrospective review of 72 patients

harboring multiple lesions at presentation. *J Neurosurg* 2002; 97(Suppl.):S511–S514.
6. Hindo WA, DeTrana FA, Lee MS, *et al.* Large dose increment irradiation in treatment of cerebral metastasis. *Cancer* 1970;26: 138–141.
7. Young DF, Posner JB, Chu F, *et al.* Rapid-course radiation therapy of cerebral metastasis: Results and complications. *Cancer* 1974;34:1069–1076.
8. DeAngelis LM, Delattre JY, Posner JB. Radiation-induced dementia in patients cured of brain metastases. *Neurology* 1989; 39:789–796.
9. Asai A, Matsutani M, Kohno T, *et al.* Subacute brain atrophy after radiation therapy for malignant brain tumor. *Cancer* 1989;63:1962–1974.
10. Ueki K, Matsutani M, Nakamura O, *et al.* Comparison of whole brain radiation therapy and locally limited radiation therapy in the treatment of solitary brain metastases from non-small cell lung cancer. *Neurol Med Chir (Tokyo)* 1996;36:364–369.
11. Cull A, Gregor A, Hopwood P, *et al.* Neurological and cognitive impairment in long-term survivors of small cell lung cancer. *Eur J Cancer* 1994;30A:1067–1074.
12. Regine WF, Scott C, Murray K, *et al.* Neurocognitive outcome in brain metastases patients treated with accelerated-fractionation vs. accelerated-hyperfractionated radiotherapy: An analysis from Radiation Therapy Oncology Group Study 91-04. *Int J Radiat Oncol Biol Phys* 2001;51:711–717.
13. Li J, Bentzen SM, Renschler M, *et al.* Regression after whole-brain radiation therapy for brain metastases correlates with survival and improved neurocognitive function. *J Clin Oncol* 2007;25:1260–1266.
14. Folstein MF, Folstein SE, McHugh PR. "Mini-Mental State": A practical method for grading the cognitive state of patients for the clinician. *J Psychiatr Res* 1975;12:189–198.
15. Sundstrom JT, Minn H, Lertola KK, *et al.* Prognosis of patients treated for intracranial metastases with whole-brain irradiation. *Ann Med* 1998;30:296–299.
16. Nagata K, Basugi N, Fukushima T, *et al.* Quantification of brain atrophy [Japanese]. *Brain Nerve* 1985;37:255–262.
17. Taylor BV, Buckner JC, Cascino TL, *et al.* Effects of radiation and chemotherapy on cognitive function in patients with high-grade glioma. *J Clin Oncol* 1998;16:2195–2201.
18. Brown PD, Buckner JC, O'Fallon JR, *et al.* Effects of radiotherapy on cognitive function in patients with low-grade glioma measured by the Folstein Mini-Mental State Examination. *J Clin Oncol* 2003;21:2519–2524.
19. Kleinberg L, Wallner K, Malkin MG. Good performance status of long-term disease-free survivors of intracranial gliomas. *Int J Radiat Oncol Biol Phys* 1993;26:129–133.
20. van Beek AP, van den Bergh ACM, van den Berg LA, *et al.* Radiotherapy is not associated with reduced quality of life and cognitive function in patients treated for nonfunctioning pituitary adenoma. *Int J Radiat Oncol Biol Phys* 2007;68:986–991.
21. Tsuruda JS, Kortman KE, Bradley WG, *et al.* Radiation effects on cerebral white matter: MR evaluation. *AJNR Am J Neuroradiol* 1987;8:431–437.
22. Nieder C, Leicht A, Motaref B, *et al.* Late radiation toxicity after whole brain radiotherapy: The influence of antiepileptic drugs. *Am J Clin Oncol* 1997;22:573–579.
23. Meyers CA, Wefel JS. The use of the Mini-Mental State Examination to assess cognitive functioning in cancer trials: No ifs, ands, buts, or sensitivity. *J Clin Oncol* 2003;21: 3557–3558.
24. Aoyama H, Tago M, Kato N, *et al.* Neurocognitive function of patients with brain metastases who received either whole brain radiotherapy plus stereotactic radiosurgery or radiosurgery alone. *Int J Radiat Oncol Biol Phys* 2007;68:1388–1395.
25. Withers HR. Biologic basis for altered fractionation schemes. *Cancer* 1985;55:2086–2095.
26. Johnson BE, Becker B, Goff WB, *et al.* Neurologic, neuropsychologic, and computed cranial tomography scan abnormalities in 2- to 10-year survivors of small-cell lung cancer. *J Clin Oncol* 1985;3:1659–1667.
27. Lee JS, Umsawasdi T, Lee YY, *et al.* Neurotoxicity in long-term survivors of small cell lung cancer. *Int J Radiat Oncol Biol Phys* 1986;12:313–321.
28. Chak LY, Zatz LM, Wasserstein P, *et al.* Neurologic dysfunction in patients treated for small cell carcinoma of the lung: A clinical and radiological study. *Int J Radiat Oncol Biol Phys* 1986;12:385–389.
29. Poettgen C, Eberhardt W, Grannass A, *et al.* Prophylactic cranial irradiation in operable stage IIIA non-small-cell lung cancer treated with neoadjuvant chemoradiotherapy: Results from a German multicenter randomized trial. *J Clin Oncol* 2007;25: 4987–4992.
30. Murray KJ, Scott C, Zachariah B, *et al.* Importance of the Mini-Mental Status Examination in the treatment of patients with brain metastases: A report from the Radiation Therapy Oncology Group protocol 91-04. *Int J Radiat Oncol Biol Phys* 2000;48:59–64.

基礎講座 —I-125密封線源による前立腺永久挿入治療—

I-125永久挿入治療へ関わろう！～物理的QAの解説～

高橋 豊[1,2]・隅田伊織[1,2]・小泉雅彦[1]・尾方俊至[1,2]・秋野祐一[1]・井上武宏[1]
1)大阪大学大学院医学系研究科放射線治療学
2)大阪大学医学部附属病院オンコロジーセンター医学物理室

はじめに

I-125永久挿入治療はわが国で2003年に認可されて以来，急速に普及している．今や国内の約90施設で4000例を超える症例の治療が行われている．しかし，わが国ではこれまで物理的なQA (Quality Assurance)に関する議論はあまり行われてこなかった．米国医学物理学会(AAPM)では小線源治療に関する物理QAガイドライン(AAPM TG56[1]，AAPM TG64[2])が発刊されているが，これらは総論的な内容にとどまり，わが国での臨床実践は困難であった．そこで，厚生労働省がん研究助成金土器屋班のもとで小線源治療の臨床に携わる医学物理士を中心としたワーキンググループが結成され，本治療の安全性と精度の保証およびわが国で今後得られる臨床エビデンスに信頼性を与えることを目的とした本邦初の物理QAガイドライン[3]が作成された．

本ガイドラインは総論的で長文の諸外国のガイドライン[1,2,4~7]を参考にしつつも，医学物理士が不足しているわが国にも適応した，格段に実用的なものとなっている．その特徴は主に以下の5点である．

1) QAプログラムは図解やQAの実例の記載で，より具体的で分かりやすい．
2) 専門知識が必要とされるQA項目に対応し，配布用検証ソフトが独自に開発された．
3) 事故防止として最低限実施すべき事項，精度向上のために実施が好ましいことの2段階にランク付けされている．
4) 業者協力を得るアクセプタンステストを重視し，詳細に記載されている．
5) 箇条書きで，簡潔な短文とし，読みやすいものにされている．

詳細は2009年12月に配布予定のガイドラインを参照していただきたい．本稿ではI-125永久挿入治療のQAに関して重要となる部分とその背景について簡単に解説する．

各章の概要

第1章　I-125永久挿入治療の概要

ここではI-125永久挿入治療の概要を示している．本治療はアクセプタンステストから始まり，コミッショニング，プレプラン・刺入，ポストプランまでのプロセスがある．それぞれの過程で物理的な関わりが必要となってくる．それぞれの過程で必要なQA項目を端的に示している．また，本治療に関しては日本泌尿器科学会の専門医と日本放射線腫瘍学会の認定医もしくは日本医学放射線学会専門医（治療：2次試験合格者）が必要条件とされている．しかし，QAの重要性を鑑み，「専門的な放射線物理学の知識を要するスタッフ，すなわち医学物理士等」による品質保証が行われることが推奨されている．

第2章　I-125永久挿入治療の物理概論

ここではI-125永久挿入治療の物理概論についてQAを行ううえで必要な最低限の解説が記載されている．I-125のエネルギーは，線源そのものからは35.5keV (γ線)および27.5keV，31.0keV (Te-特性X線)などが放出される[4]．その他，シード線源では表面を覆っている銀(Ag)やチタン(Ti)カプセルによる特性X線が放出される．このようにI-125は非常に低いエネルギー核種であるので，他の核種に比べてもより急峻な線量分布を得ることが可能であり，臨床的には有利である．しかし，物理的には非常に扱いが難しい．

Fig. 1は，過去の線量または線量計算に関わるパラメータの値の変遷を示している．これまでに3回の変化があった[4,5,8]．1回目は(1)式で示されるいわゆる古典的線量計算式から(2)式で示されるAAPM TG43式の導入による処方線量の改定である．

$$\dot{D}(r) = A_{app} f_{med} (\Gamma_\delta)_\kappa (1/r^2) T(r) \cdot \phi_{an} \quad \cdots\cdots\cdots (1)$$

ここでA_{app}はApparent activity (見かけの放射能)，f_{med}は吸収線量変換係数，$\Gamma_{\delta\kappa}$は照射線量率定数，$T(r)$：組織空気吸収係数，ϕ_{an}は非等方性定数である．

$$\dot{D}(r,\theta) = S_k \cdot \Lambda \frac{G(r,\theta_0)}{G(r_0,\theta_0)} \cdot g(r) \cdot F(r,\theta) \quad \cdots\cdots\cdots (2)$$

ここで，S_kは空気カーマ強度，Aは線量率定数(cGyh^{-1}U^{-1})，$G(r,\theta)$は幾何学定数，$g(r)$は放射状線量関数(radial dose function)，$F(r,\theta)$は非等方性関数である．

大きな違いは二つある．一つは線源強度の定義が変わった点である．古典的線量計算式では線源形状を考慮していない見かけの放射能A_{app}から線源カプセルを含めた空中での空気カーマ強度S_kに変更になったのである．これはI-125のような低エネルギー線源の場合，線源カプセルの影響が無視できないためである．その変更後も，実際にはベンダーはA_{app}でユーザーに線源を供給している．したがって，単位の変換が必要となった．そこで，AAPMではその変換係数として1.27(U/mCi)と定義した[9]．もう一つは長さを持つ線源は先端の線量が落ちる性質(非等方性)を考慮した計算になった点である．これらにより，一部の治療計画の内部パラメータは大幅に変わり，処方線量も160Gyから145Gyに変更になったのである．これを知らずに治療をすれば10%の線量誤差を生む結果となる．また，その改定によって1995年以前の臨床論文を読む場合には注意が必要である．例えば，1995年の論文で「尿道最大線量を400Gy以下にすべきである[10]」は，現在の線量計算方法でいえば「尿道線量を360Gy以下にすべきである」が正しい．

また，1999年には米国のI-125線源強度の国家標準機関であるNIST (National Institute of Standards and Technology)による空気カーマ強度の改定が行われた．すなわち，Tiカプセルから生じる4keVの特性X線の影響を除去したのである[8]．これによって線量率定数が約10%変化した．その後，TG43 update[5]が発刊され，さらに2%程度変化した．このように治療計画装置の内部パラメータもしばしば変更になった経緯があり，また，今後もありうることである．これらの変更を実臨床に反映させるかは放射線腫瘍医と相談して決定しなければならないが，医学物理士等はそのことを説明できなければならない．

第3章　超音波，ステッパー，治療計画装置のアクセプタンステスト

第3章では超音波，ステッパー，治療計画装置のアクセプタンステストについて記載した．アクセプタンステストはシステムが仕様どおりに稼働することを業者が主体となって確認するものであり，主にYes, Noで解答可能なものである．以下の点が遵守されなければならない．

1)ベンダーはアクセプタンステスト手順書を用意し，それに基づき行わなければならない．アクセプタンステストには必ずユーザーが立ち会わなければならない．

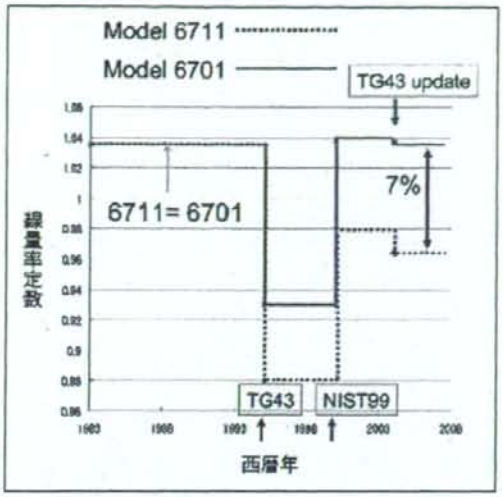

Fig. 1　線量率定数の変遷

2)アクセプタンステストの結果は文書化し，保存されなければならない．

3)新たに導入あるいはアップグレードするすべてのイメージングモダリティ，機器，治療計画システムは，アクセプタンステストを受けなければならない．

4)機種依存があるので，ここで挙げる項目に基づき，機種に応じたアクセプタンステストが実施されなければならない．

試験内容は線量計算に関するものからステッパー，超音波装置やCTのイメージの取り込みから計画装置への画像授受などの線量に関与しない試験まで幅広い．土器屋班物理QAガイドラインワーキンググループは2007年12月にアクセプタンステストの実施状況について代表的な15施設にアンケート調査を実施した．その結果，試験すら行われておらず，また試験が行われた場合であっても結果が文書化されていない施設が少数ながらあった(Fig. 2a)．アクセプタンステストは今後QAを行ううえで基準を確立するだけでなく，特に線量計算に関するテストを実施しなければ過誤照射事故につながる．すなわち，外部照射でリニアックごとのビームデータがあるように，小線源治療にも線源モデルごとの線源データが存在し，それに基づいて線量分布が作成されるのである．ベンダーは本章を参考にアクセプタンステスト試験書を準備することが望まれる．

第4章　治療計画装置のコミッショニング

コミッショニングはアクセプタンステストに引き続

き行われるユーザー主体の試験であり，すべての関連機器に対して導入時およびバージョンアップ時に行われなければならない．主に次の3点を目的とする．

1)妥当性を確認する．例えば，正しい線源データが入力されている場合に，実際に線量計算が正しく行われているかなどがそれに該当する．

2)システムをより効率的に活用するための指針を決定する．例えば，ポストプランの線源同定に有利なCT撮影条件を把握するなどがそれに該当する．

3)定期的なQCプログラムの基準を確立する．

数年前に，外部照射で過誤照射が続発したことがあったが，これは導入前のコミッショニングが行われていなかったことが主たる原因であった．小線源治療でも全く同様であり，コミッショニングは不可欠である．しかし，アンケート調査の結果，現実には30%近くの施設が全くコミッショニングを行っていないことが明らかになった(Fig. 2b)．それを回避すべく，本ガイドラインでは最低限行うべき項目を列挙した．例えば，線源データが正しく選択され，それに基づき正しく線量計算が行われていることは必ずポイント線量の独立検証により確認しなければならない．小線源治療では急峻な線量勾配が生じるため，実測による検証は困難であるので，手計算等による独立検証が推奨される．また，線量分布の検証も独立した検証がされなければならない．これらの具体的な方法はガイドライン第2章に説明されている．

事故防止だけでなく，精度の限界を把握するのもコミッショニングの一つであり，また精度の向上を図る役割も率先して果たすべきである．計算グリッドサイズがD90(90%の体積に与えられる最小線量)やV100(100%線量が与えられる体積)に及ぼす影響もコミッショニング時に検証すべきである．計算グリッドは2mmが推奨されている．治療計画装置によっては5mmがデフォルト設定されているものもある．特に頭尾方向のグリッドサイズを2mm以下にしなければ，V100やD90が最大10%程度変化する場合がある．また，ポストプラン時には自動的に線源同定をする機能がある．その精度はCT撮影条件に依存する．Fig. 3はCT撮影条件の違いによる自動線源同定精度を示している．CTスライスが厚いと部分体積効果により線源同定が困難になることが分かる．最適なCT撮影条件や自動線源同定の精度の見積もりはコミッショニング時に行われるべきである．これらのことは，治療開始後に放射線腫瘍医が試行錯誤するのではなく，事前に医学物理士等が検証し，手法を確立すべきである．

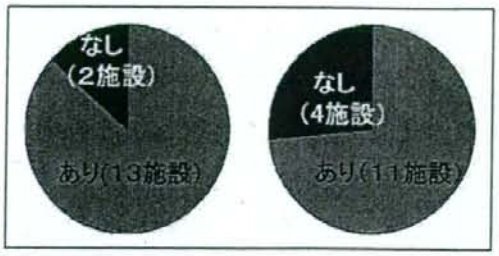

Fig. 2 アンケート結果
(a) 受け入れ試験
(b) コミッショニングの実施状況
a | b

第5章 定期的なQA

システムユニットの購入時から寿命に至るまで，購入時にできるだけ近い状態を維持するためのQCである．以下のことが遵守されなければならない．

1)QCテストの結果は文書化する．

2)装置のパフォーマンスが満たされない場合の，調整あるいは修理．早急に復旧できない場合は，臨床上許容できるか否かを判断する．

行うべきQCプログラムはDaily，Monthly，6 Monthly，Annually，Bi-annuallyで分類され，許容値とアクションレベルを示している．許容値とは検証時の精度目標を示す．またアクションレベルとは臨床で使用可能であることの目安である．すなわち，許容値以上アクションレベル以下であれば臨床使用はできるが，医学物理士は誤差原因の解明などの何らかのアクションを起こさなければならない．アクションレベルを超えた場合には治療を行ってはならない．

症例ごとに行うQCとしては医師または医学物理士等の立案した治療計画のチェック，すなわちダブルチェックをすべきである．チェック項目としては線源強度の減衰補正や線源モデルの選択，計算グリッドなどである．これらは機種によって異なるので，ガイドラインを参考にしつつ，各施設で決定していただきたい．また，線源強度の測定も重要である．米国のガイドラインAAPM TG64[2]では「少なくとも10%，理想的には全数の線源強度測定をしなければならない」と定めている．現在わが国で認可されている線源では，線源強度が十分に保証されていることが報告されている[1]．しかし，欧米の報告では業者の線源校正ミスやデッドシードの混入，過剰被ばく事故などが報告されていることも事実である．

本ガイドラインでは移行期間として強制はしていないが，本来はすべきである．実際にはマンパワーや時間の問題もあるが，これを施設でクリアされることを祈っている．その意味も込めて，第1章に「医学物

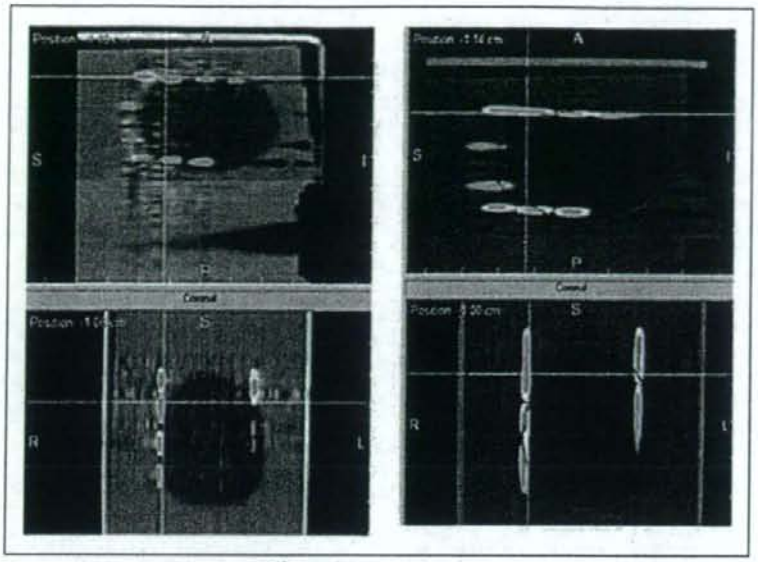

Fig. 3 CTスライス厚による自動線源同定精度
(a)1mmスライス，(b)5mmスライス
5mmスライスでは部分体積効果により正しく同定できない．

理士・品質管理士」の文言を記載している．

また，経直腸超音波(TRUS)，ステッパー，治療計画装置間のテンプレートグリッド整合性試験は円滑な刺入を行うために重要となる．もしずれていれば術者の意図と異なる場所に針が刺入されることになりうる(Fig. 4)．

第6章 放射線防護

永久挿入密封小線源を取り扱うにあたっては，関連法令に定める規制に従い線源の安全管理に努めなければならない．線源は定められた場所で適切な方法で取り扱い，保管し，作業中の被ばく軽減に努め，事故のないよう十分留意する．常に線源の所在を明らかにしておくことが重要で，想定外のアクシデントにも対処可能となる．関連事項をしっかり理解し各施設での安全管理対策マニュアルに則りそれを遵守することが大切である．これらについて解説している．また，受け入れ時の線源個数や刺入後の脱落および余剰線源の個数確認も重要である．特に，刺入後にマガジンの滅菌袋に線源が残っていた事例もあるので注意が必要である．

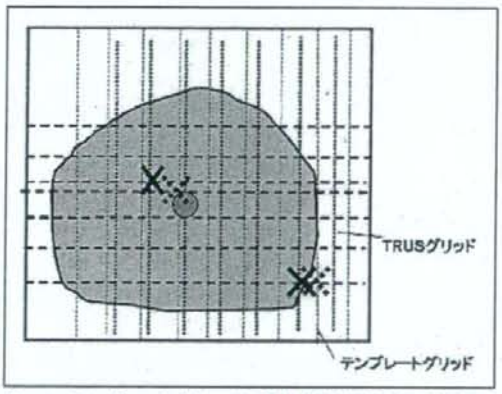

Fig. 4 テンプレートグリッドと経直腸超音波(TRUS)グリッドの整合性が取れていない場合の模式図
実際に実線×の箇所に刺入しようとしても破線×に刺入されてしまう．

おわりに

以上のように，本稿ではI-125のQAの重要性について述べた．アンケート調査結果からも何を行ってよいか分からないとの意見が多くあった．本ガイドラインはそのような要望に応える形になっている．現在のところ，医学物理士等のようなQAを行う人材が本治療にあまり関わっていない．しかし，質の高い治療と今後行われるわが国の臨床試験のエビデンスに信頼性を持たせるためにも，医学物理士や治療技師が積極的にI-125永久挿入治療に関わることを期待したい．